JOURNAL OF GEOPHYSICAL RESEARCH, VOL. 102, NO. A7, PAGES 14,407–14,414, JULY 1, 1997

Spacecraft transits across simulated field line resonance regions

W. Allan and A. N. Wright[1]

National Institute of Water and Atmospheric Research, Wellington, New Zealand

D. R. McDiarmid

Herzberg Institute of Astrophysics, National Research Council, Ottawa, Ontario, Canada

Abstract. The field line resonance (FLR) mechanism has become a cornerstone of magnetohydrodynamic wave theory in the magnetosphere and the solar atmosphere. Evidence for the mechanism comes mainly from auroral radar and geosynchronous spacecraft observations. Spacecraft in elliptical near-equatorial orbits (particularly Active Magnetospheric Particle Tracer Explorers Charge Composition Explorer (AMPTE CCE)) have seen frequency-varying oscillations of magnetic field lines but have not seen much evidence of the large-amplitude, narrowband FLRs seen by auroral radars. We simulate the resonance region of a large event observed at GOES 7 and also of a smaller-amplitude event we term a "typical Scandinavian Twin Auroral Radar Experiment (STARE) event" with reference to the STARE auroral radar results. One set of simulated narrowband FLRs is driven by a magnetopause Kelvin-Helmholtz wave. We add a fundamental continuum oscillation and analyze the resulting time series using the AMPTE CCE time-frequency analysis. We find that at the observed milliHertz frequencies the narrowband FLRs appear as large or small enhancements in the continuum of the azimuthal magnetic field but are not obviously "monochromatic." For large events, enhancements in the spectrum of the compressional magnetic component may suggest a narrowband driver. We also analyze FLRs driven by waveguide modes and find no monochromatic signatures in the compressional magnetic field.

Introduction

The magnetosphere contains a continuum of closed magnetic field shells, which may be stimulated by a broadband compressional impulse. The continuum can then execute free azimuthal oscillations, each field line (at radial position x, say) oscillating at the local Alfvén frequency $\omega_A(x)$. Such Alfvén continuum oscillations are ultimately dissipated in the ionosphere and have a lifetime τ proportional to the height-integrated ionospheric Pedersen conductivity.

A narrowband compressional source can drive part of the field line continuum into resonance at the source frequency. This Alfvén or field line resonance (FLR) concept has become a cornerstone of magnetohydrodynamic (MHD) wave theory in the magnetosphere and solar atmosphere since the original ideas were developed [*Tamao*, 1965; *Southwood*, 1974; *Chen and Hasegawa*, 1974; *Ionson*, 1978]. In a magnetospheric context the theory was stimulated by observations using latitudinal magnetometer chains [e.g., *Samson et al.*, 1971] and was apparently confirmed by auroral radar observations of resonance regions in the ionosphere [*Walker et al.*, 1979]. Proposed FLR drivers include the Kelvin-Helmholtz instability at the magnetopause boundary [e.g., *Samson et al.*, 1971; *Southwood*, 1974], magnetospheric global (cavity) modes stimulated by solar wind disturbances [e.g., *Kivelson and Southwood*, 1985; *Allan et al.*, 1985], and waveguide modes on the magnetospheric flanks [e.g., *Walker et al.*, 1992; *Wright*, 1994].

Whilst there is general agreement upon what is meant by a resonance for an ideal (dissipationless) system in which everything oscillates at a single frequency in the steady state, there is no such consensus for a time-dependent system. Since real ULF pulsations are time dependent and dissipative, it seems worthwhile to try and generalize the definition of a resonance and to decide if a specific field line is in resonance or not. We begin by addressing a related, but better posed, ques-

[1]On leave from Mathematical Institute, University of St Andrews, Fife, Scotland.

Paper number 97JA01082.
0148-0227/97/97JA-01082$09.00

tion: On which field lines will large-amplitude Alfvén waves (LAWs) be excited as a response to fast-mode driving?

We offer the following criterion for the establishment of LAWs: A general driver will have a frequency spectrum characterized by a central frequency ω_d and a bandwidth $\Delta\omega_d$ (which can be a function of time and x). The bandwidth will arise from both modulation and finite duration of the driver or from the fact that the driver may contain irregular or random oscillations. The bandwidth may be very broad, say $\Delta\omega_d/2 \sim \omega_d$. Each field line will have a natural eigenfrequency that will in general be complex, because of ionospheric dissipation. The frequency spectrum of a freely decaying Alfvén oscillation (of complex frequency) at position x will have a central frequency equal to the real part of its eigenfrequency (i.e., the continuum frequency $\omega_{Ar}(x)$), and a width ($\Delta\omega_A(x)$) equal to twice the damping rate, $\Delta\omega_A(x) = 2\omega_{Ai}(x)$. A LAW will grow on the field line at x if the driving spectrum ($\omega_d - \Delta\omega_d/2 \rightarrow \omega_d + \Delta\omega_d/2$) and the Alfvén spectrum for that field line ($\omega_{Ar}(x) - \Delta\omega_A(x)/2 \rightarrow \omega_{Ar}(x) + \Delta\omega_A(x)/2$) overlap.

It is instructive to consider some simple limits of our LAW criterion, and we begin with the clearest:

1. An ideal system which has been driven for an infinite time by a steady driver of constant frequency ω_d will have $\Delta\omega_d = \Delta\omega_A = 0$, so the only field line that fulfills the LAW requirement is the field line for which $\omega_A(x) = \omega_d$. This field line corresponds to a singularity and is also the familiar "textbook" definition of a resonance.

2. A system with a dissipative ionosphere which has been driven for an infinite time by a steady driver of constant frequency will have $\Delta\omega_d = 0$, $\Delta\omega_A \neq 0$. All transients will have decayed, and only motions at the driving frequency (ω_d) remain. A layer of field lines between x_1 and x_2 supports LAWs (where $\omega_{Ar}(x_1) + \Delta\omega_A(x_1)/2 = \omega_{Ar}(x_2) - \Delta\omega_A(x_2)/2 = \omega_d$). The finite width of a dissipative "resonance" is a familiar result [e.g., *Southwood and Hughes*, 1983; *Wright and Allan*, 1996].

3. An ideal system which has been driven coherently for a finite time or by an incoherent driver (time limited or not) will have $\Delta\omega_d \neq 0$, $\Delta\omega_A = 0$. A layer of field lines between x_1 and x_2 supports LAWs (where $\omega_{Ar}(x_1) + \Delta\omega_d/2 = \omega_{Ar}(x_2) - \Delta\omega_d/2 = \omega_d$). The field lines oscillate at their natural frequencies and also the frequency components of the driver. Note that the incoherent driver corresponds to the situation described by *Hasegawa et al.* [1983].

4. A system with a dissipative ionosphere which has been driven coherently for a finite time or by an incoherent driver (time limited or not) will have $\Delta\omega_d \neq 0$, $\Delta\omega_A \neq 0$. A layer of field lines between x_1 and x_2 supports LAWs (where $\omega_{Ar}(x_1) + \Delta\omega_A(x_1)/2 + \Delta\omega_d/2 = \omega_{Ar}(x_2) - \Delta\omega_A(x_2)/2 - \Delta\omega_d/2 = \omega_d$). Oscillations will decay in time and will be dominated at time t by the frequency components of the driver over the interval $t - \tau \rightarrow t$ (τ is the ionospheric decay time). In this case $\Delta\omega_d$ should be calculated over just the preceding interval τ.

If the driver is very broadband, the layer of field lines supporting LAWs in the last two cases may be very wide. Although a specific field line will oscillate with all the frequency components of the driver, they are weighted by a factor of approximately $1/(\omega^2 - \omega_A^2)$ so that those driving frequency components close to the natural frequency will dominate the response. In practice this means that the frequency spectrum of an incoherently driven field line will have a peak centered upon the natural Alfvén frequency of that field line. This feature can apparently be seen in the Active Magnetospheric Particle Tracer Explorers (AMPTE) spectrograms of *Engebretson et al.* [1986]. However, the observational situation is complicated by the fact that oscillations close to the natural Alfvén frequency can exist for a time much longer than τ if the continuum is driven by random broadband compressional waves either continually or as impulses spaced on average a time $\sim \tau$ apart. In the latter case the continuum oscillations would decay typically by a factor of only $1/e$ before being stimulated again. Observationally, it may be difficult to distinguish between such intermittently driven long-duration continuum oscillations and LAWs driven continually by modulated incoherent broadband sources.

Note that case 4 includes all observable events, since in practice there will always be some ionospheric dissipation and a time-limited driver.

It is evident from the above discussion that there are many similarities between field lines supporting LAWs and resonant field lines. For example, in case 1 the two definitions are interchangeable. However, there is no (exact) equivalence in the other cases. Part of the problem comes from there being no universally accepted precise definition of a resonance in the more general cases. A reasonable definition of a resonant field line would be to say that the resonant singularity occurred on it. This will be fulfilled when the driving frequency matches the (in general complex) Alfvén frequency. For case 2 (a dissipative system with $\Delta\omega_d = 0$, $\Delta\omega_A \neq 0$) there is no resonant singularity, and one could justifiably claim that no field lines are resonant. However, this goes against textbook usage where the field line for which $\omega_{Ar}(x) = \omega_d$ is commonly termed "resonant." In a very real sense this field line is no different to any others: it simply responds to the fast wave by generating an Alfvén wave with amplitude proportional to the factor $1/(\omega_d^2 - \omega_A^2)$. The field line is only special in the sense that it maximizes this factor but otherwise is just like any other field line. Consequently, we could argue that if the $\omega_{Ar}(x) = \omega_d$ field line is to be termed "resonant," then so should all field lines, as they are all equal and none contain any singularities!

Despite our rather pedantic discussion of exactly what is meant by the term resonance, it is clear that in common parlance the situation in case 2 is regarded as a resonance. We are happy to adopt this, arguably imprecise, usage. Indeed, we will go further and for simplicity refer to all the situations above in which field lines support LAWs as "field line resonances" (FLRs) throughout the rest of this paper. We will also refer to

a field line resonance driven by a narrowband source as a "narrowband FLR."

As mentioned earlier, ground-based radar observations [e.g., *Walker et al.*, 1979; *Poulter*, 1982] appeared to show clear signatures of relatively large-amplitude, spatially narrow FLR regions. These strongly suggested the existence of narrowband drivers of significant duration. Based on such observations, *Engebretson et al.* [1986] and *Anderson et al.* [1989] expected to see obvious narrowband resonance regions when they analyzed magnetometer data from the AMPTE Charge Composition Explorer (CCE) elliptically orbiting spacecraft. Instead, their time-frequency plots for complete orbits of the spacecraft showed power in the azimuthal magnetic component at what appeared to be harmonics of the fundamental Alfvén frequency $\omega_A(L)$ as the spacecraft traversed L shells. There was little evidence of narrowband excitation. This has continued to be the case with further analysis of the AMPTE CCE data set [e.g., *Engebretson et al.*, 1987; *Anderson et al.*, 1990; *Takahashi and Anderson*, 1992; *Anderson and Engebretson*, 1995].

The existence of FLRs driven by narrowband sources has been inferred from multiple geosynchronous spacecraft [e.g., *Hughes et al.*, 1978]. Recent simultaneous observations of Pc 5 ultralow frequency (ULF) wave events using the GOES 7 geosynchronous satellite and the Canadian Auroral Network for the OPEN Program Unified Study magnetometer array have provided convincing evidence that the events studied were indeed narrowband FLRs observed at different positions within the resonance region [*Ziesolleck et al.*, 1996].

We consider ground-based observations to be as important as spacecraft observations. Discrepancies between ground-based and certain geosynchronous spacecraft data on the one hand, and elliptically orbiting spacecraft data on the other, must be explained if we are to claim understanding of the underlying physics. Here we intend to explore the above anomaly by simulating elliptically orbiting spacecraft transits across numerically modeled FLR regions driven by narrowband sources and by analyzing the results using a method as similar as possible to the AMPTE CCE time-frequency analysis. This allows us to determine how both large-amplitude and typical narrowband FLR regions should appear on AMPTE CCE time-frequency plots. We also analyze (using the same method) the DE 1 spacecraft transit through twin waveguide resonances as simulated by *Rickard and Wright* [1995].

Model Time Series

Kelvin-Helmholtz-Driven Waves

To simulate narrowband FLR regions for comparison with GOES 7 and Scandinavian Twin Auroral Radar Experiment (STARE) observations, we use the numerical model described by *Allan et al.* [1985, 1986], referred to from now on as the AWP model. We feel that, on the basis of lack of observational confirmation, global cavity modes (as opposed to waveguide modes) do not seem to be significant drivers of narrowband FLRs in the outer magnetosphere. We assume that the GOES 7 events [*Ziesolleck et al.*, 1996] were driven by short-duration evanescent compressional waves originating in the outer magnetosphere, and we consider that the Kelvin-Helmholtz instability at or near the magnetopause probably is still as good an explanation as any for the origin of the driving waves. At the magnetopause of the AWP model, we impose an oscillating electric field E_A in the azimuthal direction, with growth and decay chosen to simulate a particular observed event. This driver is taken to represent a situation in which the magnetopause becomes briefly Kelvin-Helmholtz unstable and then stabilizes again.

As a benchmark, we choose the event of March 26, 1990 (1335 to 1435 UT), shown in Figures 7 and 8 of *Ziesolleck et al.* [1996] (ZFM from now on). This event occurred near 0800 magnetic local time (MLT) during a period of fairly high magnetic activity when GOES 7 was at a magnetic latitude of $\lambda = 9°$. The 2.8 mHz frequency of the wave at $L \simeq 6.7$ (invariant latitude $\sim 67°$) is consistent with frequencies measured in the ionosphere at this latitude using STARE [e.g., *Poulter et al.*, 1984, Figure 2]. The long period implies a fundamental standing wave structure along the magnetic field line, and the total amplitude of about 7 nT must be considered large for a fundamental standing wave at only 9° away from the equatorial plane. This is confirmed by the large total amplitude of ~ 300 nT measured at the ground magnetometer station Gill (Figure 8 of ZFM).

The driving electric field function for this event (made complex to establish a clear azimuthal propagation) is shown in Figure 1, the simulation being run for 30 normalized time units. The normalized driver frequency was chosen to give a resonance position at $L = 6.7$. A dimensionless azimuthal wavenumber $m = 4$ was taken, consistent with the measurements of ZFM. A reasonable L^{-4} density variation in the equatorial plane was also chosen. To simulate the observed event a large ionospheric damping decrement $\kappa = 0.15$ was required. The model was run at high resolution, with 2000 radial grid points, equivalent to a grid spacing of $\Delta L = 0.005$.

Figure 2 shows the radial, azimuthal, and field-aligned magnetic field components (B_R, B_A, B_F) generated by

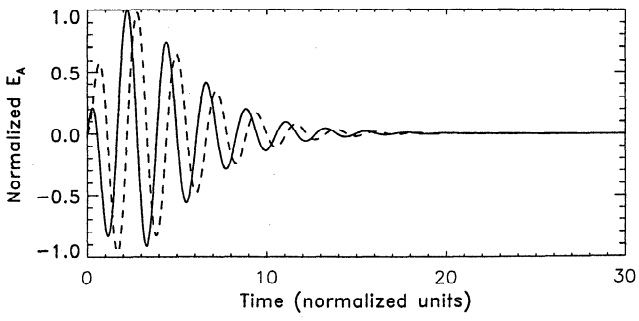

Figure 1. The Kelvin-Helmholtz driver applied in the azimuthal electric field at the magnetopause boundary. The real and imaginary parts are shown by solid and dashed lines, respectively.

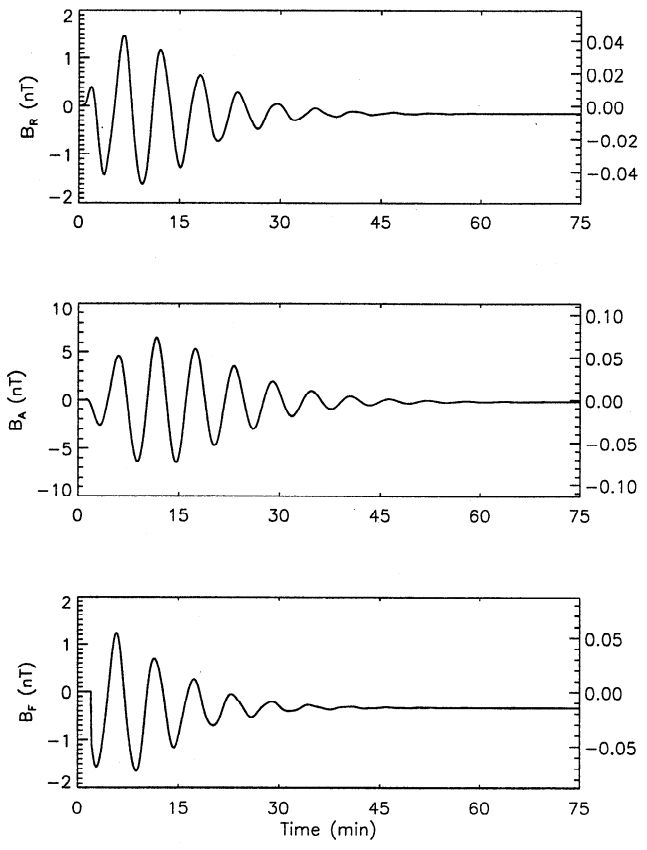

Figure 2. The radial (B_R), azimuthal (B_A), and field-aligned (B_F) magnetic components near the center of the resonance in the simulation of the GOES 7 event of 1335 to 1435 UT, March 26, 1990. These should be compared with the left-hand panels in Figure 7 of *Ziesolleck et al.* [1996]. The labels on the right-hand axes of Figure 2 show the normalized amplitudes obtained from the simulation before scaling individually to the GOES 7 observation.

the model near the resonant field line. The time unit has been scaled so that the model wave period is consistent with the GOES 7 wave period. Note that low-pass filtering of B_F was required to remove a small but noticeable fundamental cavity mode component occurring because the model magnetopause is a reflector after the driver dies away. The narrowband FLR associated with this cavity mode lay at a position well inside the Kelvin-Helmholtz-driven resonance. In reality, cavity modes are probably removed by leakage out of the magnetosphere.

The numbers on the right-hand axes in Figure 2 show the normalized amplitudes of the components given by the simulation. The left-hand axes show the components scaled individually to the amplitudes of the observed components. The ratio B_A/B_F is significantly smaller in the simulation than in the observation. We attribute this to the difference in equilibrium field geometry between the simulation model and the real magnetosphere. Our main purpose is to obtain a detailed resonance structure in L rather than a completely consistent model, so we retain the independent scaling of the components to the observation.

The March 26, 1990, GOES 7 event was the largest of the set of events chosen for the ZFM study. We estimate that it was roughly twice as large at the ground as the largest of the STARE events described by *Walker et al.* [1979]. Other STARE events described by *Walker et al.* [1979] were a factor of about 3 smaller than the largest STARE event. We have therefore generated what we term a "typical STARE event" which has an amplitude a factor of 5 less than the GOES 7 event and also has $\kappa = 0.05$, which we consider to be a more typical damping decrement. The Kelvin-Helmholtz driver in this case was similar to that in Figure 1 but with somewhat longer duration. The wave component time series for this model event are shown in Figure 3. The total amplitude of ~ 1.5 nT at $\lambda = 9°$ was comparable with many of the events selected for the ZFM study, although they were not necessarily at the same λ value.

Spacecraft Time Series

To generate the spacecraft time series we need to "fly" a spacecraft through the simulated resonance region. For the spacecraft trajectory we use a least squares fit to the L and time values given by *Anderson et al.* [1989]. It is a good enough approximation to take the spacecraft as remaining at $\lambda = 9°$ during the resonance transit.

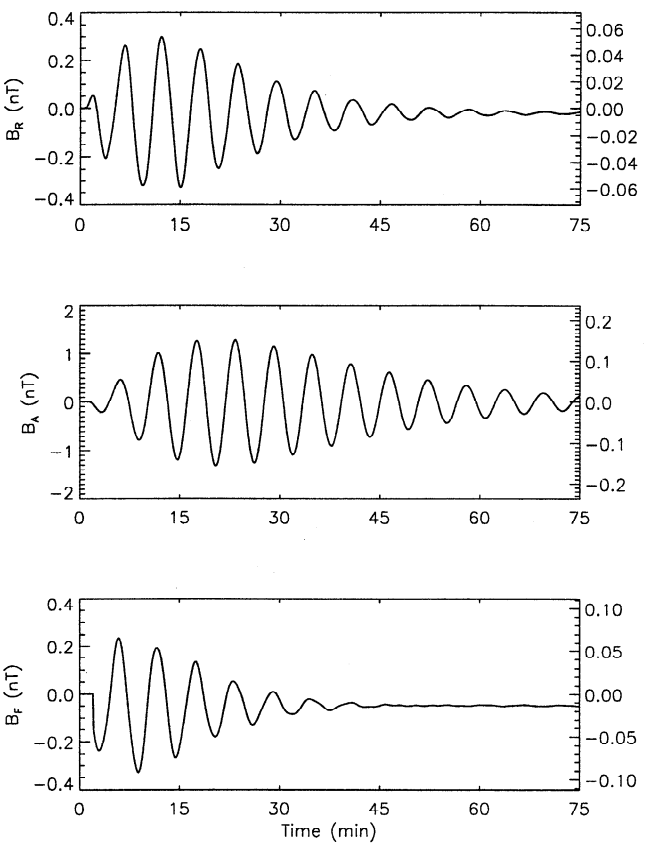

Figure 3. As in Figure 2, but for the typical STARE event simulation.

We also assume that the effect of spacecraft azimuthal motion is not significant [*Anderson et al.*, 1989]. We generate a set of time series for the three magnetic field components through the resonance region at 61 L values from $L = 6.25$ to $L = 7.75$ with a spacing of $5\Delta L$ (which was found to be sufficient spatial resolution for the spacecraft transit). The number of points in the time series is chosen so that when $\Delta t = 6.24$ s (the time increment of the AMPTE CCE data) the period of the waves in the model time series at the central field line of the narrowband FLR is consistent with the wave period in the GOES 7 event. L values for these time series points are then generated from the fitted spacecraft trajectory. Finally, "snapshots" of the wave magnetic amplitudes in L at each time point are made, and the amplitudes at each spacecraft L value are interpolated from these snapshots.

The AMPTE CCE data which *Anderson and Engebretson* [1995] term "harmonic intervals" contain oscillations with continuously varying frequency in the B_A component that can be present at all L values. We simulate these by generating an oscillation with the same continuously varying period as used in the narrowband FLR simulation, and add this to the B_A time series for the regions $L < 6.25$ and $L > 7.75$. *Anderson et al.* [1989] described the temporal form of their continuum data in terms of "ringing times," suggesting that the data could well consist of a sequence of short impulses separated by intervals in which the waveform partially decays. This was supported by the observed small accumulation of phase shear which suggested that the phase of the frequency-varying oscillations was being impulsively reset after a relatively small number of cycles. We avoid the introduction of large phase shear frequency distortion [*Anderson et al.*, 1989] by resetting the phase of the oscillations every 3 cycles and also allow the oscillations to decay with an e-folding time of about 4 cycles. These values are roughly consistent with the results of *Anderson et al.* [1989]. Our frequency-varying oscillation is effectively generated by a sequence of compressional impulses and can be considered as a "sustained continuum" oscillation. The resulting ringing field lines decay through ionospheric dissipation in rough accord with the ringing times described in Table 3 of *Anderson et al.* [1989]. Note that the frequency-varying oscillations observed could actually be the result of a sustained incoherent driver, but we feel that in either case the visual result in the AMPTE CCE time-frequency plots will be similar.

We take the maximum amplitude of our continuum oscillation to be 0.7 nT, this being an estimate of the maximum likely frequency-varying amplitude in the 0 to 10 mHz band based on the published AMPTE CCE time-frequency plots. The AMPTE CCE data contain noise in this frequency band of about 0.2 nT amplitude during active times (M. J. Engebretson, personal communication, 1995). Ambient noise in the spacecraft environment has a $1/f$ frequency distribution. We therefore add $1/f$-distributed noise to the time series for all three magnetic components, the amplitude of this noise in the 0 to 10 mHz band being approximately 0.2 nT. We also include a small proportion of uniformly distributed noise to represent magnetometer digitization noise [*Takahashi et al.*, 1990]. Note that we are only concerned with fundamental standing modes here and have not included higher harmonics in the B_A component at present. To represent the repeated impulsive compressional stimuli which drive our continuum, we have included a suitable proportion of uniformly distributed power in the B_R and B_F components. Note that the continuum, noise, and compressional power we have added to the modeled narrowband FLR fields are not intended to conform to any detailed theoretical model but are designed to give a realistic background in the time-frequency plots against which the oscillations driven by a narrowband source can be compared.

Figure 4 shows the complete B_A component time series for the GOES 7 and typical STARE events. In the top panel the resonance region for the large GOES 7 event stands out obviously from the continuum, but the typical STARE event is not so obvious. Note that the spacecraft trajectory has been chosen such that the spacecraft passes through the resonance center at the time of maximum FLR amplitude. The results given below therefore show the maximum amplitudes observable for these modeled events.

We also employ the AMPTE CCE analysis on the simulated DE 1 transit through two waveguide FLRs described by *Rickard and Wright* [1995], using the waveguide simulation of *Rickard and Wright* [1994]. We interpolate the time series given in Figure 9 of *Rickard and Wright* [1995] to the 6 s time increment

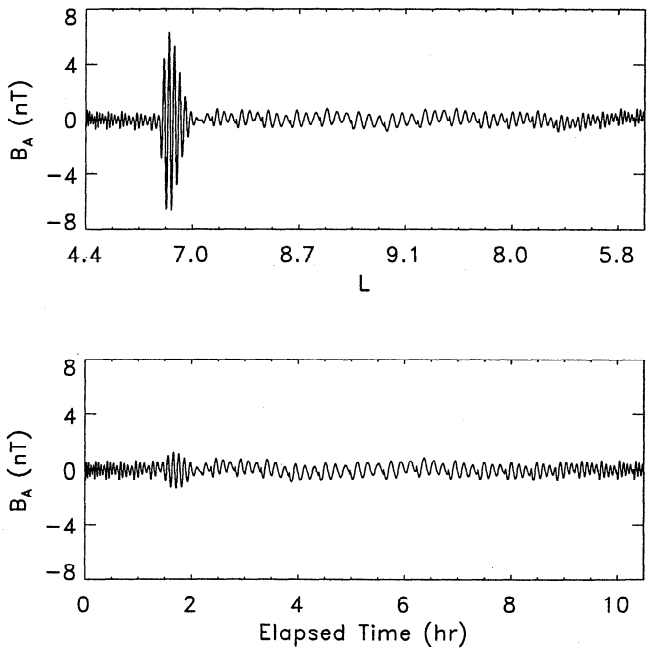

Figure 4. Complete azimuthal magnetic fields for the spacecraft transits of the (top) simulated GOES 7 event and (bottom) simulated typical STARE event after addition of the fundamental mode continuum and noise components.

of the DE 1 spacecraft magnetometer. No continuum or noise is added to the time series in this case.

Analysis and Results

We follow as closely as possible the AMPTE CCE analysis described by *Engebretson et al.* [1986] and *Anderson et al.* [1989]. The data (spaced at intervals of 6.24 s) are first differenced and then transformed by applying a 256 point fast Fourier transform using a 10% cosine taper window. This window is shifted successively by 40 time points through the complete time series, and the resulting power spectra are plotted versus time and L value of the spacecraft. The spectra are scaled to ensure that, for example, a spectral intensity of 10^{-3} nT^2 Hz corresponds to 0.4 nT amplitude at 5 mHz and 0.1 nT at 20 mHz [*Anderson et al.*, 1989]. This inverse dependence of amplitude on frequency results from the data differencing [*Takahashi et al.*, 1990]. Differenced data then have uniform noise when the original data have $1/f$ noise. Since the continuum harmonic amplitudes also tend to vary roughly as $1/f$, differencing enhances the visibility of the higher harmonics in time-frequency plots. Conversely, differencing tends to visually de-emphasize the fundamental frequency relative to the higher harmonics in those plots.

In Figure 5 we display an outward and inward spacecraft passage, including a transit through the GOES 7-like narrowband FLR around $L = 6.7$. The spectrum of the continuum fundamental mode is reasonably clear against the background noise in the 0 to 10 mHz band of the azimuthal magnetic component. The large-amplitude azimuthal FLR stands out against the continuum but appears as a major intensification of the continuum rather than as a clearly monochromatic structure superimposed on the continuum. This occurs partly because the time-dependent nature of the event means that the azimuthal component is not purely monochromatic but mainly because the relatively short duration does not allow a clear distinction between narrowband and continuum (broadband) components.

The other magnetic components in Figure 5 stand out more clearly because there is no continuum, although their intensity is significantly less than that of the azimuthal component. It is possible that one could deduce from the complete picture in Figure 5 that the enhancement of the continuum is a narrowband FLR driven by a quasi-monochromatic fast wave.

We consider that the GOES 7 event modeled in Figure 5 is a large-amplitude example and that events of this size should occur infrequently. We feel that the typical STARE event shown in the bottom panel of Figure 4 is more representative of the size of event that AMPTE CCE should have passed through more commonly. Figure 6 shows the spacecraft transit through the typical STARE event. In the azimuthal component there is a barely discernible intensification of the continuum and faint patches in the other magnetic components which could easily be overlooked if the slight continuum intensification were not noticed.

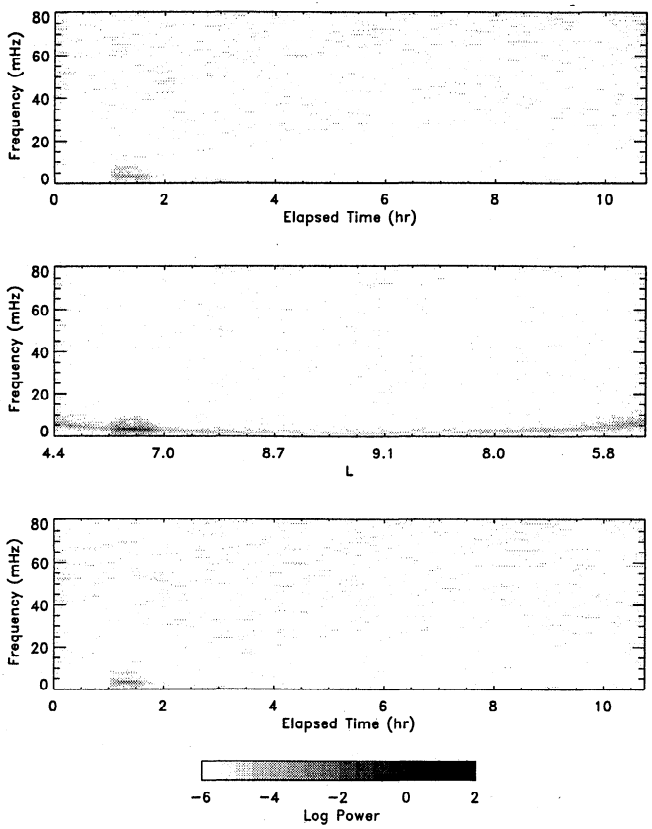

Figure 5. AMPTE CCE time-frequency analysis of the (top) radial, (middle) azimuthal and (bottom) field-aligned magnetic components for the simulated GOES 7 event. Equivalent L values are shown in the middle panel.

Figure 7 shows the results of the AMPTE CCE analysis applied to the waveguide simulation data shown in Figure 9 of *Rickard and Wright* [1995], representing a transit of the DE 1 spacecraft [*Lin et al.*, 1992] through the FLR regions. The model has two FLRs at $L \simeq 10.3$ and 7.7. The azimuthal magnetic component shows an apparent continuum with two enhancements which would be hard to confirm as "monochromatic." The main point to note is that, at this stage of the development of the waveguide mode structure, there is nothing in the field-aligned (or compressional) component that would suggest monochromatic drivers, as pointed out by *Rickard and Wright* [1995]. The radial component in Figure 7 also has little evidence of monochromatic structure. If the events in Figures 5 and 6 had been driven by waveguide sources rather than Kelvin-Helmholtz or ideal cavity mode sources, the discrete patches in the radial and field-aligned components would not have occurred, and we would have been left with only large or small enhancements of the continuum as evidence of the narrowband FLRs.

Conclusions

We have simulated narrowband FLR regions driven by short-duration Kelvin-Helmholtz-like drivers using the cylindrical model of *Allan et al.* [1985, 1986]. By

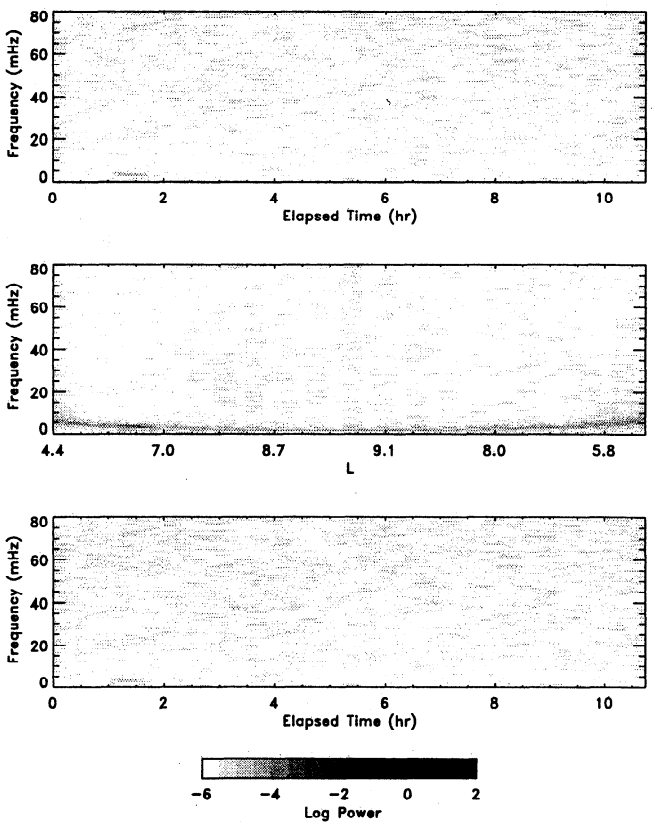

Figure 6. As in Figure 5, but for the typical STARE event.

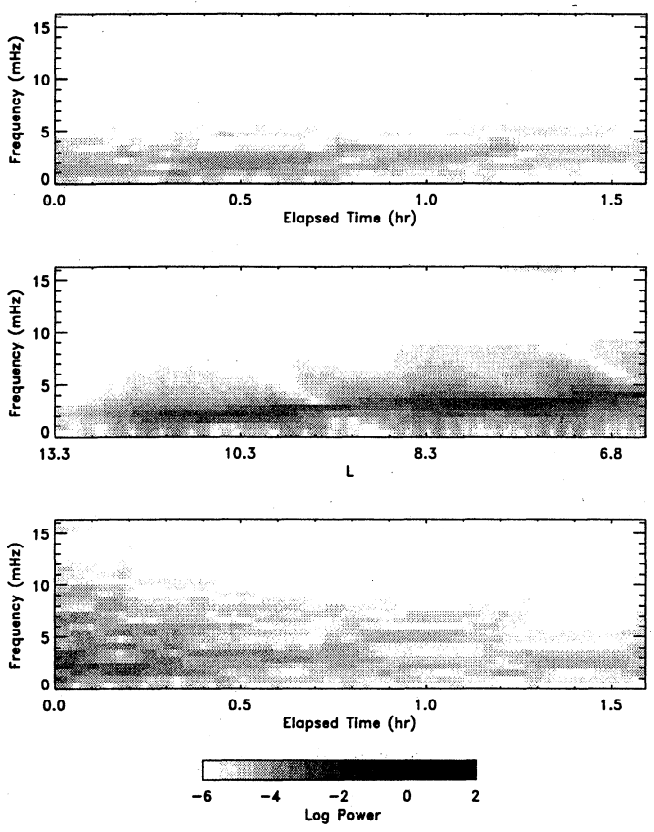

Figure 7. AMPTE CCE analysis of the DE 1 waveguide resonance transit [*Rickard and Wright*, 1995]. Equivalent L values are shown in the middle panel.

varying the duration of the driver and the effective ionospheric damping, we have simulated a particular large-amplitude event observed at GOES 7. Comparing the relative amplitudes of the magnetic field components at GOES 7 and in the simulation shows that, if the GOES 7 event was indeed a narrowband FLR, the real magnetospheric geometry apparently enhances the ratio of Alfvén to compressional wave amplitude relative to the simulation. The ionospheric damping decrement was also large ($\gamma/\omega \simeq 0.15$).

By scaling the magnetic field components individually to the GOES 7 observations, we created a model resonance region which was then traversed by a spacecraft to give time series equivalent to an AMPTE CCE transit of the resonance. These time series were extended to simulate an outward and inward passage of AMPTE CCE by adding a fundamental mode continuum oscillation (effectively driven by repeated compressional impulses) in the azimuthal magnetic field, with appropriate noise in all three components. The final time series were analyzed using the AMPTE CCE time-frequency technique.

The large-amplitude GOES 7 event showed a strong enhancement of the continuum around the resonance position, but this was not obviously "monochromatic" when compared with the continuum variation. Weaker patches appeared at the resonance position for the other components, perhaps allowing interpretation as a fast mode driving the narrowband FLR if all three components were considered. We feel that such a large-amplitude event would seldom have been encountered by AMPTE CCE.

A smaller-amplitude narrowband FLR was also simulated, termed a "typical STARE event" by comparison with the majority of events observed using the STARE radar [*Walker et al.*, 1979]. We consider that AMPTE CCE should have encountered such events relatively often. However, the analysis showed only a weak enhancement of the continuum at the resonance position and very faint patches in the other components. Such events would be difficult to identify as narrowband FLR regions from the AMPTE CCE time-frequency analysis.

We also applied the AMPTE CCE analysis to a simulation of a DE 1 spacecraft transit through waveguide resonance regions [*Rickard and Wright*, 1995]. The resonance regions were clearly seen but were not obviously monochromatic. Also the other magnetic components (particularly the compressional component) did not contain a signature at any particular frequency. If the GOES 7 and typical STARE events described above had been driven by waveguide modes, their "monochromatic" nature would have been even less obvious.

To sum up, the identification of clearly monochromatic FLR regions at frequencies of less than 10 mHz is not an easy task using the AMPTE CCE data and time-frequency analysis technique. This is first because the elliptical orbit of AMPTE CCE does not allow the generation of high-resolution frequency spectrograms dur-

ing the transit of such a resonance region, and second because typical fundamental mode narrowband FLRs should have relatively small amplitude near the magnetospheric equatorial plane, although generally larger than the fundamental continuum (or broadband response) amplitude.

Acknowledgments. We thank a referee for useful comments which have improved this paper. W.A. acknowledges support by the New Zealand Foundation for Research, Science and Technology (FRST) through contract CO1627. W.A. also thanks E. M. Poulter for helpful discussions. A.N.W. is supported through a UK PPARC Advanced Fellowship and is grateful to PPARC and FRST for funding his visit to NIWA, New Zealand.

The Editor thanks David Southwood and Brian J. Anderson for their assistance in evaluating this paper.

References

Allan, W., S. P. White, and E. M. Poulter, Magnetospheric coupling of hydromagnetic waves – Initial results, *Geophys. Res. Lett., 12,* 287, 1985.

Allan, W., S. P. White, and E. M. Poulter, Impulse-excited hydromagnetic cavity and field-line resonances in the magnetosphere, *Planet. Space Sci., 34,* 371, 1986.

Anderson, B. J., and M. J. Engebretson, Relative intensity of toroidal and compressional Pc 3–4 wave power in the dayside outer magnetosphere, *J. Geophys. Res., 100,* 9591, 1995.

Anderson, B. J., M. J. Engebretson, and L. J. Zanetti, Distortion effects in spacecraft observations of MHD standing waves: Theory and observation, *J. Geophys. Res., 94,* 13,425, 1989.

Anderson, B. J., M. J. Engebretson, S. P. Rounds, L. J. Zanetti, and T. A. Potemra, A statistical study of Pc 3–5 pulsations observed by the AMPTE CCE magnetic fields experiment, 1, Occurrence distributions, *J. Geophys. Res., 95,* 10,495, 1990.

Chen, L., and A. Hasegawa, A theory of long-period magnetic pulsations, *J. Geophys. Res., 79,* 1024, 1974.

Engebretson, M. J., L. J. Zanetti, and M. H. Acuna, Harmonically structured ULF pulsations observed by the AMPTE CCE magnetic field experiment, *Geophys. Res. Lett., 13,* 905, 1986.

Engebretson, M. J., L. J. Zanetti, T. A. Potemra, W. Baumjohann, H. Lühr, and M. H. Acuna, Simultaneous observation of Pc 3–4 pulsations in the solar wind and in the Earth's magnetosphere, *J. Geophys. Res., 92,* 10,053, 1987.

Hasegawa, A., K. H. Tsui, and A. S. Assis, A theory of long period magnetic pulsations, 3, Local field line oscillations, *Geophys. Res. Lett., 10,* 765, 1983.

Hughes, W. J., R. L. McPherron, and J. N. Barfield, Geomagnetic pulsations observed simultaneously on three geostationary satellites, *J. Geophys. Res., 83,* 1109, 1978.

Ionson, J. A., Resonance absorption of Alfvénic surface waves and the heating of solar coronal loops, *Astrophys. J., 226,* 650, 1978.

Kivelson, M. G., and D. J. Southwood, Resonant ULF waves: A new interpretation, *Geophys. Res. Lett., 12,* 49, 1985.

Lin, N., M. J. Engebretson, L. A. Reinleitner, J. V. Olson, D. L. Gallagher, L. J. Cahill, J. A. Slavin, and A. M. Persoon, Field and thermal plasma observations of ULF pulsations during a magnetically disturbed interval, *J. Geophys. Res., 97,* 14,859, 1992.

Poulter, E. M., Pc 5 micropulsation resonance regions observed with the STARE radar, *J. Geophys. Res., 87,* 8167, 1982.

Poulter, E. M., W. Allan, J. G. Keys, and E. Nielsen, Plasmatrough ion mass densities determined from ULF pulsation eigenperiods, *Planet. Space Sci., 32,* 1069, 1984.

Rickard, G. J., and A. N. Wright, Alfvén resonance excitation and fast wave propagation in magnetospheric waveguides, *J. Geophys. Res., 99,* 13,455, 1994.

Rickard, G. J., and A. N. Wright, ULF pulsations in a magnetospheric waveguide: Comparison of real and simulated satellite data, *J. Geophys. Res., 100,* 3531, 1995.

Samson, J. C., J. A. Jacobs, and G. Rostoker, Latitude-dependent characteristics of long-period geomagnetic micropulsations, *J. Geophys. Res., 76,* 3675, 1971.

Southwood, D. J., Some features of field line resonances in the magnetosphere, *Planet. Space Sci., 22,* 483, 1974.

Southwood, D. J., and W. J. Hughes, Theory of hydromagnetic waves in the magnetosphere, *Space Sci. Rev., 35,* 301, 1983.

Takahashi, K., and B. J. Anderson, Distribution of ULF energy ($f < 80$ mHz) in the inner magnetosphere: A statistical analysis of AMPTE CCE magnetic field data, *J. Geophys. Res., 97,* 10,751, 1992.

Takahashi, K., B. J. Anderson, and R. J. Strangeway, AMPTE CCE observations of Pc3–4 pulsations at $L = 2$–6, *J. Geophys. Res., 95,* 17,179, 1990.

Tamao, T., Transmission and coupling resonance of hydromagnetic disturbances in the non-uniform Earth's magnetosphere, *Sci. Rep. Tohoku Univ. Ser. 5, 17,* 43, 1965.

Walker, A. D. M., R. A. Greenwald, W. F. Stuart, and C. A. Green, STARE auroral radar observations of Pc 5 geomagnetic pulsations, *J. Geophys. Res., 84,* 3373, 1979.

Walker, A. D. M., J. M. Ruohoniemi, K. B. Baker, R. A. Greenwald, and J. C. Samson, Spatial and temporal behavior of ULF pulsations observed by the Goose Bay HF radar, *J. Geophys. Res., 97,* 12,187, 1992.

Wright, A. N., Dispersion and wave coupling in inhomogeneous MHD waveguides, *J. Geophys. Res., 99,* 159, 1994.

Wright, A. N., and W. Allan, Structure, phase motion and heating within Alfvén resonances, *J. Geophys. Res., 101,* 17,399, 1996.

Ziesolleck, C. W. S., Q. Feng, and D. R. McDiarmid, Pc 5 ULF waves observed simultaneously by GOES 7 and the CANOPUS magnetometer array, *J. Geophys. Res., 101,* 5021, 1996.

W. Allan, National Institute of Water and Atmospheric Research, P. O. Box 14-901, Kilbirnie, Wellington, New Zealand. (e-mail: w.allan@niwa.cri.nz)

D. R. McDiarmid, Herzberg Institute of Astrophysics, National Research Council, Ottawa, Ontario, Canada K1A 0R6. (e-mail: mcdiarmid@dan018.dnet.sp-agency.ca)

A. N. Wright, Mathematical Institute, University of St. Andrews, St Andrews, Fife KY16 9SS, Scotland. (e-mail: andy@dcs.st-and.ac.uk)

(Received September 30, 1996; revised March 17, 1997; accepted April 9, 1997.)